Available online at www.sciencedirect.com
ScienceDirect
Polymer 47 (2006) 7988–7996
polymer
www.elsevier.com/locate/polymer

Structure and piezoelectric properties of poly(vinylidene fluoride) studied by density functional theory

Zhi-Yin Wang [a], Hui-Qing Fan [a,*], Ke-He Su [b,*], Zhen-Yi Wen [c]

[a] School of Materials Science and Engineering, Northwestern Polytechnical University, Xi'an, Shaanxi 710072, China
[b] Department of Applied Chemistry, School of Natural and Applied Sciences, Northwestern Polytechnical University, 127 West YouYi Road, Xi'an, Shaanxi 710072, China
[c] Institute of Modern Physics, Northwest University, Xi'an, Shaanxi 710068, China

Received 2 June 2006; received in revised form 1 September 2006; accepted 3 September 2006
Available online 29 September 2006

Abstract

The internal rotation, geometry, energy, vibrational spectra, dipole moments and molecular polarizabilities of poly(vinylidene fluoride) (PVDF) of α- and β-chain models were studied by density functional theory at B3PW91/6-31G(d) level. The effects of chain lengths and monomer inversion defects on the electric properties and vibrational spectra were examined. The results show that the *tgtg′* conformation angle between *g* and *g′* is about 55° and the *ttt* conformation is a slightly distorted all-*trans* alternating planar zigzag with ±175° repeating motif. The average distance between adjacent monomer units in the β-PVDF is 2.567 Å. The energy difference between the α- and β-chains is about 10 kJ/mol per monomer unit. The dipole moment will be affected by chain curvature (with a radius of about 30.0 Å for ideal β-chain) and by defect concentration other than localization. The chain lengths and defects will not significantly affect the mean polarizability. The calculations indicated that there are some additional characteristic vibrational modes that may help identification of the α- and β-phase PVDF.

Keywords: DFT; PVDF; Polymer physical chemistry

1. Introduction

Recently, polymers have received more attention as new ferroelectric or piezoelectric materials than ceramic-based materials [1–13]. The advantages are well known by their unique features, such as large strain without structure fatigue, light weight, low cost, great mechanical strength, easy processability into thin and flexible films of various shapes and sizes, and most importantly, flexible architecture design via molecular tailoring. Therefore, the discovery of piezoelectricity in poly(vinylidene fluoride) (PVDF), [H–$(CH_2–CF_2)_n$–H], firstly reported by Kawai in 1969 [1], has attracted a great deal of attention for potential applications [2,3]. Within the last decades, PVDF has been widely investigated on its important pyro- and piezoelectric properties [4–6]. Many of them have been employed in practical applications [3,7–11], e.g. ultrasound transducer in nondestructive evaluation and medical ultrasound [6,12,13].

PVDF is well known for its polymorphism. Five crystal phases with different conformations are all-*trans* (*ttt*) planar zigzag β-phase, *tgtg′* (*g* denotes *gauche* form) α- and δ-phases, and $t_3g t_3g'$ γ- and ε-phases [8,14]. Since the C–F bond is a polar bond with typical dipole moment of $\mu = 6.4 \times 10^{-30}$ C m [15], the all-*trans* conformation has the highest dipole moment ($\mu = 7.0 \times 10^{-30}$ C m) per unit due to the alignment of all dipoles in one direction [16]. If the polymer chains pack into crystals with parallel dipoles, the crystal possesses a net dipole moment such as in the cases of polar β-, γ- and δ-phases. Whereas, if they do with anti-parallel

* Corresponding authors. Tel.: +86 29 88493915; fax: +86 29 88493325 (K.-H.S); tel./fax: +86 29 88494463 (H.-Q.F.).
E-mail addresses: hqfan3@163.com (H.-Q. Fan), sukehe@nwpu.edu.cn (K.-H. Su).

0032-3861/$ - see front matter © 2006 Elsevier Ltd. All rights reserved.
doi:10.1016/j.polymer.2006.09.016

dipoles the net dipole moment vanishes as in the cases of non-polar α- and ε-phases. Among these phases, the β-phase has the highest spontaneous polarization in a unit crystal cell [17]. The large value of unit cell polarization for an oriented and polarized sample is from the closer packing of polymer chains in a unit cell. Therefore, the polar β-phase has shown technological interest in obtaining excellent properties of pyro- and piezoelectrics. Although this phase can be obtained by different techniques [18–23] (among those, the most important one being the polarization under mechanical stretching of α-phase films to a certain percent at a given temperature [21–23]), the mechanisms of phase stability and phase transitions are not clearly understood.

From molecular structure point of view, important factors affecting the electrical properties of PVDF include chain length (or molecular weight distributions [24]), crystallization phases, and inverted monomer unit defects. Among them the defect concentration of PVDF is typically on the order of 5%. Its effect on the crystallization behavior had been studied before [25]. Defects may be included in the crystallites if the thickness of lamellas is larger than their average distance apart. However, the degree of crystallization decreases with increasing defect concentration. For understanding the structure–property relationship, theoretical investigations were carried out using semi-empirical quantum mechanical methods, empirical molecular dynamics simulations (MDS) and ab initio quantum mechanical methods. Hasegawa et al. [26] reported that the total potential energy difference between the α- and β-phases is 0.3 kcal/mol by MDS. Using MDS, Takahashi [27] predicted that the polar β-phase crystal is unstable without long-range electrostatic interaction. He suggested that electrostatic interaction controls the stability of the spontaneous polarization in the ferroelectric phase of PVDF. On the basis of Hartree–Fock (HF) calculations and experimental phonon frequencies, Karasawa and Goddard [28] reported energy differences among four different polymorphs of PVDF (including α- and β-phases). Their results are within 1 kcal/mol per monomer. They have also established two force fields for MDS and predicted PVDF structures and properties. Li et al. [29] calculated the β-chain (containing 11 monomer units) of PVDF by HF/STO-3G and forecasted that the dipole moment per monomer unit would increase if the length of polymer chain increases. Wang et al. [30,31] calculated the vibrational modes of β-chain with 11 monomer units using HF/3-21G method. They proposed that frequencies in the 1330–1020 cm^{-1} range might be responsible for the spontaneous polarization. Farmer et al. [32], using MD potentials to determine the chain conformation and packing energies, confirmed that conversions between the α- and β-phases should be energetically feasible, but increasing the concentration of head-to-head defects in PVDF would favor the formation of β-phase. Correia and Ramos [33] studied the effect of both chain length and monomer inversion defect on electrical properties of individual PVDF by a method combining MDS with a self-consistent semi-empirical quantum mechanical method. They predicted that the contribution of monomer unit to dipole moment of the polymer has different outcome (it would decrease for α- and increase for β-PVDF, but either of them will converge to a constant), and the dipole moment would decrease with increasing defect concentration.

From reviewing of literature, it is clear that many investigators believe energies due to short-range non-bonded interactions determine the stability of different PVDF phases [34,35]. For example, Furukawa concluded that the β-phase is primarily stabilized by the *van der Waals* interaction, and the coulomb interaction causes instability [34] based on the potential energies of PVDF calculated by Hasegawa et al. [26]. Tashiro and Kobayashi suggested that intramolecular steric repulsion between non-bonded fluorine atoms might be one of the most important factors governing the transition behavior of fluorine polymers based on the stability of the *trans* and *gauche* conformations in the ferroelectric phase transition of the related copolymers [35]. However, energies calculated by the previous studies have significant errors because of the crude approximations in the empirical and semi-empirical quantum mechanical methods applied. Thus it is desirable to re-examine the issue using more reliable state-of-the-art quantum mechanical methods. In this study, we performed calculations on internal rotation potentials, geometries, and electrical properties of α- and β-PVDF chains by using the first principle density functional theory (DFT) at B3PW91/6-31G(d) level of theory. For different conformations, energy differences, permanent dipole moment, molecular polarizability per monomer, and vibrational spectra were obtained. The effects of chain length and monomer inversion defects on electrical properties and vibrational spectra of the α- and β-chains were examined. Characteristic vibrational modes of the α- and β-chains were assigned and compared with the experimental spectra.

2. Theoretical method

The advent of density functional theory has provided an alternative means for including electron correlations in the study of moderately large molecules [36–39]. In our previous systematic comparisons [40,41], a number of theoretical methods including DFT at BPW91, B3LYP and B3PW91 levels of theory, second order Møller–Plesset perturbation theory (MP2), and quadratic configuration interaction at QCISD and QCISD(T) levels with basis sets ranging from 6-31G(d,p) to 6-311G(2d,p) levels, have been examined for geometry optimizations for all of the first and second row inorganic molecules collected in the CRC Handbook of Chemistry and Physics [42]. It was shown that B3PW91 reproduces the equilibrium structures systematically better than the other methods. We therefore employed B3PW91 (a combination of the Becke's three-parameter (B3) exchange functional [43] and the correlation functional of Perdew and Wang, PW91 [44]) in the current study. To balance accuracy and computational cost, 6-31G(d) (valence double ξ plus *d* polarization functions on heavy atoms) basis sets was used. The Gaussian-03 package [45] was used for all the calculations. We did not use *p* polarization functions for hydrogen atoms so that we can use established frequency scaling factor [46,47]. Calculations were performed for internal rotation

potentials, geometry optimizations and vibration analyses of PVDF α- and β-chain with different lengths as well as molecular energy and dipole moment vectors (μ_x, μ_y, μ_z). For vibrational analyses, the molecular exact polarizability tensors, α_{xx}^{mol}, α_{xy}^{mol}, α_{yy}^{mol}, α_{xz}^{mol}, α_{yz}^{mol} and α_{zz}^{mol}, were obtained, which, e.g. α_{xy}^{mol}, is defined as the linear response to an externally applied electric field [48]:

$$\mu_x^{ind} = \alpha_{xy}^{mol} E_y^{ext}$$

where μ^{ind} is the induced molecular dipole moment, E^{ext} is the magnitude of the applied electric field and x, y, z represent the Cartesian components. For vibrational assignments, B3PW91/6-31G(d) frequencies were scaled by scaling factor 0.9573 [46,47].

3. Results and discussion

3.1. Internal rotation

The internal rotation of PVDF chains is a key step for transition from one phase into another. Farmer et al. [32] reported an energy barrier of about 10 kcal/mol by an empirical potential calculation. The barrier calculated by our B3PW91/6-31G(d) is about 16.3 kJ/mol for the α → β transition in a two-monomer-units model $H(CH_2CF_2)-(CH_2CF_2)H$ as shown in Fig. 1. The rotation begins and ends up at C–C–C–C *cis*-conformation (denoted as 0° and 360°). It is interesting to note that present energy barrier is much smaller than that in Ref. [32]. It is also shown in Fig. 1 that our calculated β → α transition energy barrier is 8.2 kJ/mol, almost half of the value in Ref. [32].

In an X-ray crystallography investigation, Hasegawa et al. [26] proposed that the α-phase is a distorted *tgtg′* structure with a carbon dihedral repeating motif of 45°. Lando and coworkers [49,50] agreed with the Hasegawa conformation but pointed out that statistical packing plays a role and proposed a more 'ideal' *tgtg′* conformation with *g* and *g′* angles of about 60°. Hasegawa et al. also proposed that the β-phase conformation is a slightly distorted all-*trans* alternating planar *zigzag* with an alternating ±172° repeating motif [26]. The present work (Fig. 1) shows that the *tgtg′* conformation (α-chain) between *g* and *g′* angle is about 55° and the β-chain conformation is a slightly distorted all-*trans* alternating planar *zigzag* with ±175° repeating motif. For β-chain, the present result is close to that of Hasegawa et al. [26]. For α-conformation, it is in between the values of Lando and coworkers [49,50] and Hasegawa et al. [26]. As shown in Fig. 1, the all-*trans* "idea β-chain conformation" (with a carbon dihedral angle of ideal 180°) is actually a transition state (confirmed by frequencies analysis) in the path of internal rotation with very small energy barrier of about 0.1 kJ/mol, predicting that the carbon dihedral repeating motif of β-chain conformation would be actually in an arbitrary angle at around 180°.

3.2. Geometry and stability

As shown in Fig. 2(a), the chains containing 2–21 monomer units (using ideal β-chain with C_s symmetry) were examined in this study. The results indicate that the average distance of adjacent monomer units decreases with increasing chain length and converges to a nearly constant value of 2.567 Å. It is in excellent agreement with the experimental value of 2.56 Å from X-ray diffraction [51]. This result implies that the method employed in this work is quite reliable. The distances between the adjacent fluorine couples are almost a constant with an average value of 2.674 Å. Those between the adjacent hydrogen couples are also nearly a constant, but the average value is 2.482 Å, smaller than that between adjacent fluorine couples, predicting that the chain must be bent into a circular structure as shown in Fig. 5(c).

The average energy differences, $(E_\beta - E_\alpha)/n$, between α- and β-chain PVDFs are shown in Fig. 2(b) for chains containing 5–20 monomer units ($n = 5$–20). It is shown that the energy

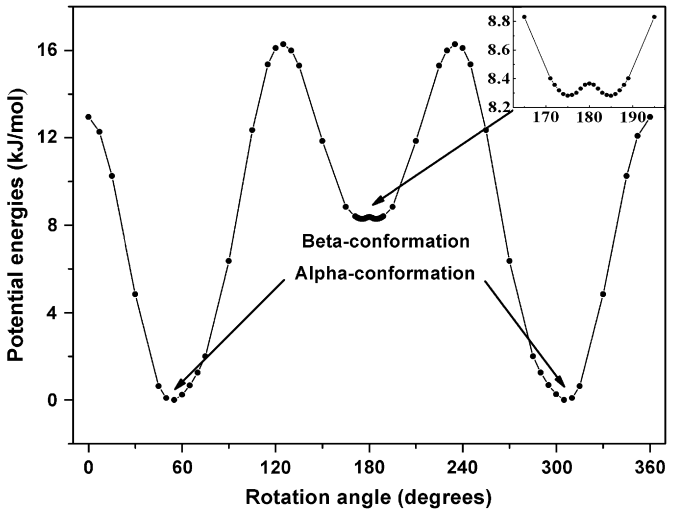

Fig. 1. Internal rotation potential energy curve of PVDF chain units in $H(CH_2CF_2)-(CH_2CF_2)H$.

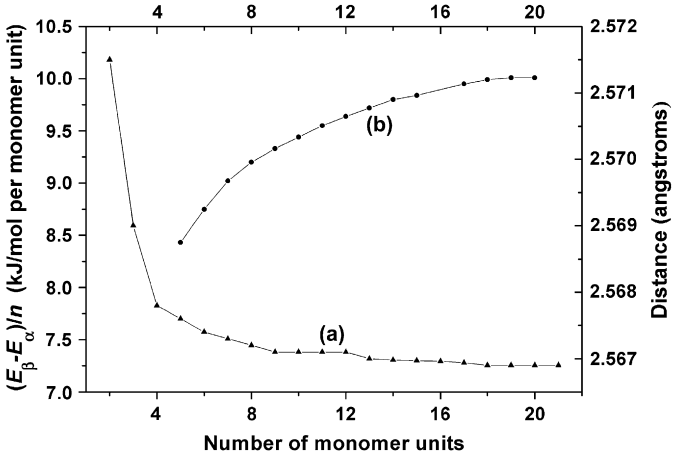

Fig. 2. (a) Average distances of adjacent monomer unit vs. chain lengths of β-PVDF (right-hand axis) and (b) energy differences per monomer unit between α- and β-PVDF chains $[H-(CH_2-CF_2)_n-H]$ ($(E_\beta - E_\alpha)/n$) vs. chain lengths (left-hand axis).

difference increases with increasing chain length and converges to a nearly constant value of about 10 kJ/mol. The magnitude is obviously larger than those from literature (from 0.3 [26] to 1 kcal/mol [28]) obtained by MDS. This suggests that the α-chain might be even more stable than previous predictions. This may explain why it is necessary to subject PVDF film to severe mechanical stretching and electric poling to prepare polar β-phase [21–23].

3.3. Dipole moment and mean polarizability

Determined by conformation, stability of molecular aggregate, electrical dipole and polarizability, the electrical response properties are of fundamental importance in piezoelectricity polymers. Since a typical polymer contains molecular chains with some statistical distribution of chain length and in order to examine the effects of chain length on the electrical properties of PVDF, we calculated the average permanent dipole moment $\mu = (\mu_x^2 + \mu_y^2 + \mu_z^2)^{1/2}/n$ and the mean polarizabilities $\alpha = (\alpha_{xx} + \alpha_{yy} + \alpha_{zz})/3n$ [48] for different chain lengths (n units) as shown in Figs. 3 and 4. It is shown in Fig. 3 that contribution per monomer unit decreases with increasing chain length for both β- and α-chains. The magnitude is about −1.2% per monomer in the β-chain. This is because the dipole moment in individual monomer unit is perpendicular to the chain and the chain is curved, mainly due to electrostatic repulsion between F atom couples on one side as shown in Fig. 5(c). The curvature radius for the chains containing 6–20 monomer units is almost a constant of about 30.0 Å (actually within a very small range of 29.8–30.9 Å). This result for β-chain PVDF is different from that obtained by the empirical MDS [33], where the chain was predicted to be in beeline and consequently the dipole contribution per monomer unit was a constant. The magnitudes of contribution to the 20 units model are 3.81×10^{-30} C m for α- and 5.01×10^{-30} C m for β-chain. Thus, one of the most important means for achieving higher spontaneous polarization is to force the polymer chains in beeline by mechanical stretching.

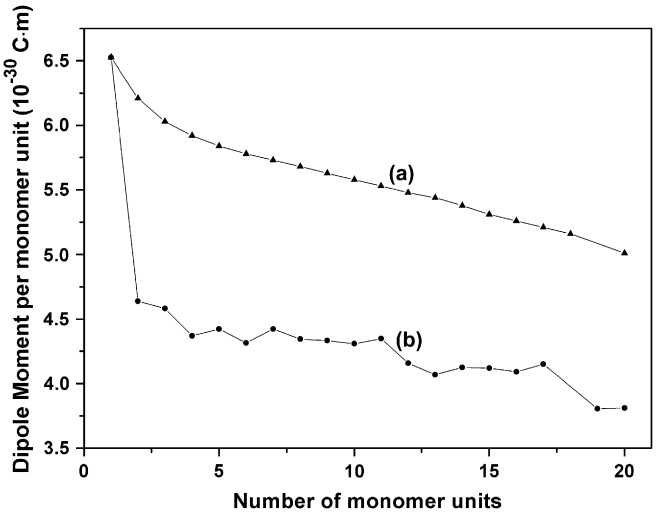

Fig. 3. Dipole moment per monomer unit vs. PVDF chain length: (a) β-chain and (b) α-chain.

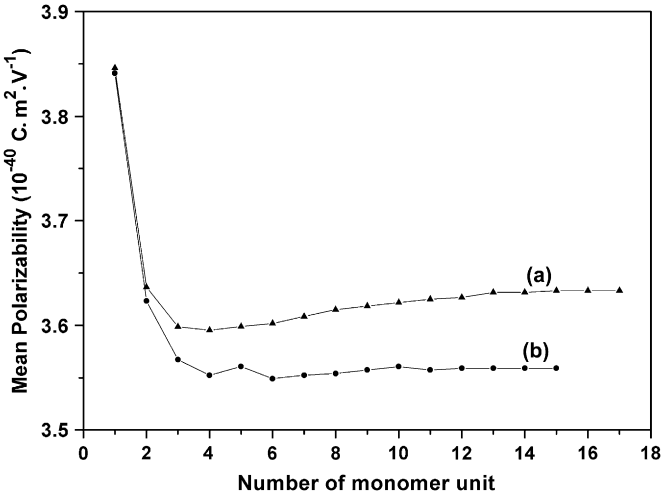

Fig. 4. Mean polarizability per monomer unit vs. the PVDF chain length: (a) β-chain and (b) α-chain.

For a single monomer unit in β-PVDF chain, which eliminates the value reduction from chain curvature, the dipole moment is calculated to be 6.53×10^{-30} C m as shown in Fig. 3. This is in excellent agreement with the value of 6.4×10^{-30} [15] and 7.0×10^{-30} C m [16] (evaluated with all unit dipoles in one direction), but is smaller than the result obtained from CNDO calculations of 8.3×10^{-30} C m [33].

Fig. 4 shows that the mean polarizability per monomer unit in β-PVDF is slightly higher than that in α-PVDF. Chain length does not seem to produce a significant effect on the mean polarizability for either α- or β-PVDF. The mean polarizabilities per monomer unit are 3.56×10^{-40} C m^2 V^{-1} for α- and 3.63×10^{-40} C m^2 V^{-1} for β-PVDF.

3.4. Inversion monomer defects

The effect of inversion monomer defects in both α- and β-chains on electrical properties of PVDF is examined for polymer chains having 15 and 20 monomer units with 1–3 inverted monomer units. The optimized structures of α- and β-chains with three inverted units and without inverted monomer unit defects are shown in Fig. 5. The positions of the three inverted units in the 20-monomer α- and β-chains are marked by arrows in Fig. 5(b) and (d). The molecular dipole moments are shown in Fig. 6 and the polarizabilities are shown in Fig. 7.

Fig. 6 plots the molecular dipole moments of α- and β-PVDF chains with 15 and 20 monomer units vs. the number of inverted monomer unit defects located at the *end* (*e*), in the *middle* (*m*), and at an arbitrary *isolated* (*i*) position of the chain. It is shown that for both chain lengths, the dipole moment of α- and β-PVDFs decreases with increasing defect concentration but the dipole moment is not significantly affected by defect locations. Typical numerical results are listed in Table 1. They show that molecular dipole moment

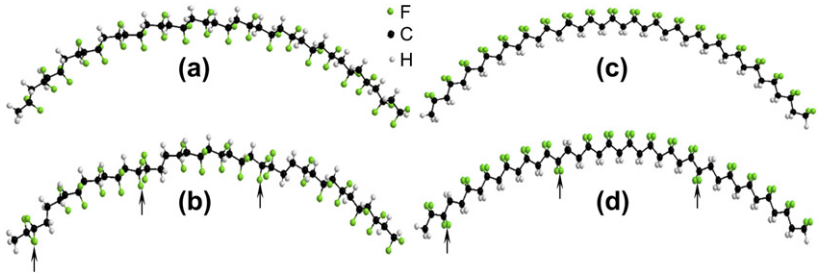

Fig. 5. B3PW91/6-31G(d) optimized structures of 20-monomer PVDF: (a) defect-free α-chain, (b) α-chain containing three isolated inversion monomer defects, (c) defect-free β-chain, and (d) β-chain containing three isolated inversion monomer defects. The arrows indicate the position of the inversion monomer defects.

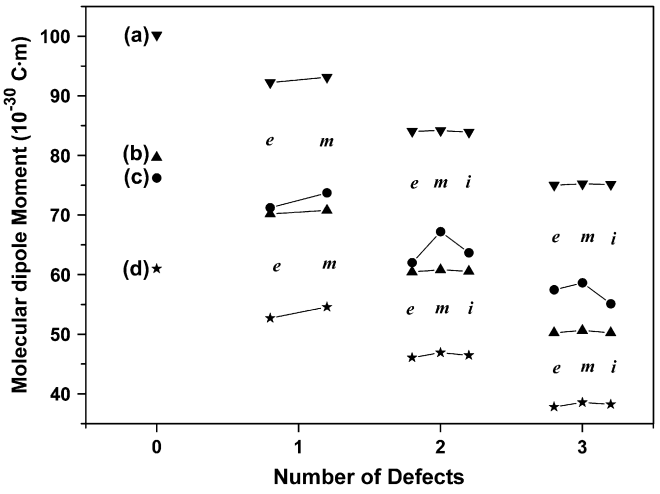

Fig. 6. Molecular dipole moments of α- and β-chain PVDFs vs. the number of inverted monomer units and their positions (*e*, *m* and *i* denote the defect located at the *end*, in the *middle* and at *isolated* position(s) of polymer chains, respectively): (a) down triangle denotes β-chain with 20 monomer units, (b) up triangle denotes β-chain with 15 monomer units, (c) closed marks denotes α-chain with 20 monomer units, and (d) pentacle marks denotes α-chain with 15 monomer units. The lines are a guide to the eye.

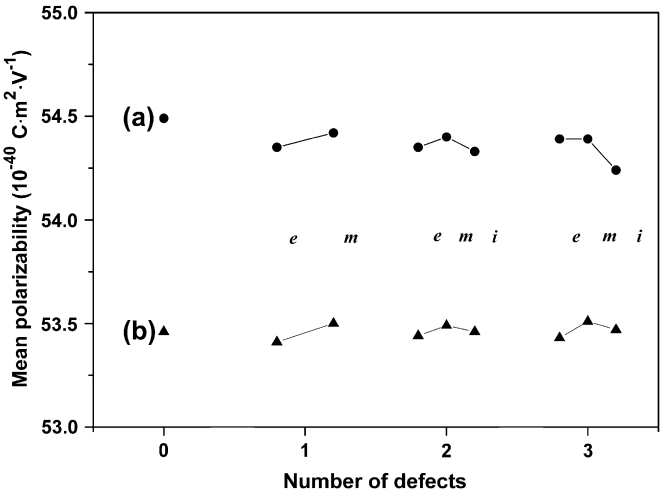

Fig. 7. Molecular mean polarizability of PVDF chains with 15 monomer units vs. the number of defects: (a) closed marks indicates β-chain and (b) trigonal marks indicates α-chain. (*e*, *m* and *i* denote the defect located at the *end*, in the *middle* and at *isolated* position(s) of polymer chains, respectively).

is reduced with increasing defects concentration for both chain lengths.

Fig. 7 plots the molecular mean polarizability of polymer chain (with 15 monomer units) as a function of the number of defects for both α- and β-PVDF. It shows that neither the defect location nor concentration has significant impact for the molecular mean polarizability of the α-chain. The presence of inverted monomer units slightly decreases the value of β-chain.

3.5. Vibrational spectra

The vibrational spectra for both α- and β-chain PVDF with 5–15 monomer units, with and without defect(s), were

Table 1
Magnitudes of molecular dipole moments for different chain lengths and defect concentrations

Number of monomer units	α-Chain PVDF			β-Chain PVDF		
	n[a]	$\mu/(10^{-30}$ C m)	$(\Delta\mu/\mu)\times 100$[b]	n[a]	$\mu/(10^{-30}$ C m)	$(\Delta\mu/\mu)\times 100$[b]
15	0	60.98	0.0	0	79.66	0.0
	1	54.57	−10.5	1	70.79	−11.1
	2	46.50	−23.7	2	60.56	−24.0
	3	38.20	−37.4	3	50.24	−36.9
20	0	76.20	0.0	0	100.23	0.0
	1	73.73	−3.3	1	93.12	−7.1
	2	63.68	−16.4	2	83.93	−16.3
	3	55.12	−27.7	3	75.16	−25.0

[a] Denotes the number of defects, $n=1$ for one defect in the middle of the polymer chains, and $n=2$–3 for defects at isolated positions.
[b] Denotes the percentage of dipole moment reduced.

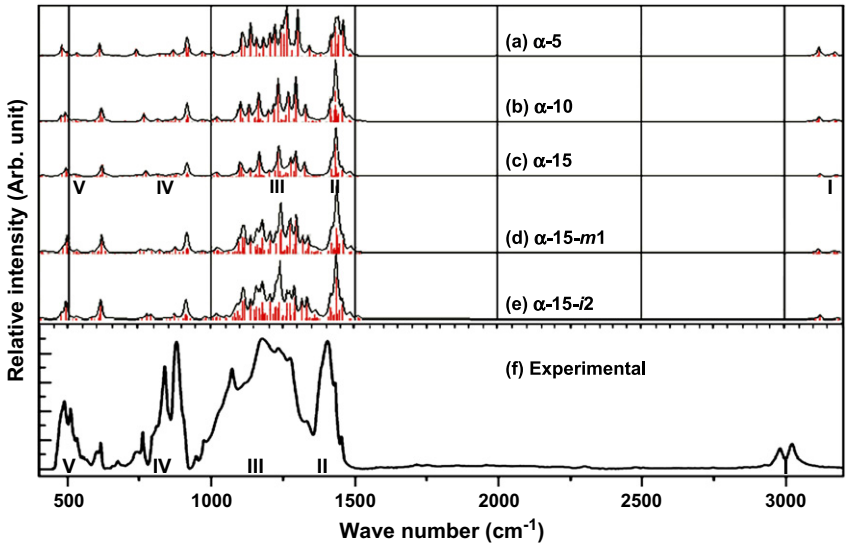

Fig. 8. Calculated IR spectra of α-chain PVDF by B3PW91/6-31G(d): (a) 5 monomer units, (b) 10 monomer units, (c) 15 monomer units, (d) 15 monomer units with one inverted monomer unit defect located in the *middle* of the chain, (e) 15 monomer units with two *isolated* inverted monomer unit defects, and (f) experimental.

calculated. Some of the infrared vibrational spectra of α-PVDF are shown in Fig. 8. Fig. 8(a)–(c) are the simulated spectra for chains having 5, 10 and 15 monomer units, respectively. Fig. 8(d) and (e) are the simulated spectra for chains with 15 monomer units having 1–2 inverted monomer unit defects. Fig. 8(f) is the experimental spectrum (Aldrich catalog No. 18270-2, CAS Number 24937-79-9, av. MW ca. 53,4000, film by *N*,*N*-dimethylformamide casting, resolution 2 cm^{-1}, Thermo Nicolet Co.).

Comparison shows that the calculated spectra are in good agreement with experiments, especially in the regions of 1085–1500 cm^{-1}. The spectra can be divided into five bands denoted in Roman numbers in the diagram for convenience of discussion.

From the results of our calculations, we can make detailed vibrational assignment for some of the observed bands in experimental spectrum. Band **I** is from C–H stretching mode with relative weak IR intensities. The calculated frequencies are about 150 cm^{-1} higher than experimental. This is a well-known [47] deficiency of theoretical calculations. Band **II** with higher relative intensity corresponds to C–H rocking modes, the calculated frequency range 1398–1500 cm^{-1} matches experimental result 1362–1462 cm^{-1} very well. Band **III** covers a larger range (1000–1350 cm^{-1}, bandwidths $\Delta = 350\ cm^{-1}$) and is consistent with experiments (930–1340 cm^{-1}, $\Delta = 410\ cm^{-1}$) as well as previous calculations [31]. CH twisting and wagging modes are responsible for this band. Although the calculated intensities in the frequency range of 1085–1350 cm^{-1} match the experiments well, those in the range of 1000–1085 cm^{-1} are significantly lower than experiments. This difference may be from the defects in the commercial PVDF as shown in (d) and (e). Bands **IV** (760–950 cm^{-1}, $\Delta = 190\ cm^{-1}$ in (c), and 760–920 cm^{-1} in (f)) and **V** (450–640 cm^{-1}, $\Delta = 190\ cm^{-1}$ in (c), and 460–620 cm^{-1} in (f)) are the vibrational modes mainly from the $-CH_2$ and $-CF_2$ rocking and skeletal bending. The inherent frequencies of α-PVDF at 525 (CF_2 bending), 616 and 772 cm^{-1} (CF_2 bending and skeletal bending) are in excellent agreement with the experimental observations (530, 615 and 765 cm^{-1}, respectively) [52]. Fig. 8(d) and (e) shows that the introduction of defects has improved the theoretical spectrum in bands **II** and **III**, making them more close to the observations. The improvement becomes more evident with higher defect concentration. Therefore, the broadening (with respect to (c)) of the bands may be largely due to the localized modes associated with inversion monomer defects [53,54] in the commercial PVDF.

Fig. 9 shows the simulated IR spectra of β-chain PVDF. Fig. 9(a)–(c) is the spectra for chains having 5, 10 and 15 monomer units, respectively. Fig. 9(d) and (e) are the spectra of 15 unit chains having 1 and 2 inverted monomer unit defects, respectively. Fig. 9(f) is the partial spectra of (c) in the range of 830–890 cm^{-1}.

The IR spectra for different chain length and inverted monomer units in β-chains are similar to those of the α-chains. The most distinguishable vibrational modes are found in bands **III**, **IV** and **V**. In band **III**, peaks at 1347 and 1288 cm^{-1} have the highest intensity. The 1347 cm^{-1} mode corresponds to all of the C^F (C bonded to F atoms) atoms symmetrically moving in-plane and perpendicular to the polymer chain. The 1288 cm^{-1} mode corresponds to all of the out-of-plane $-CH_2$ twisting and C–F bond stretching (only C^F moving in the CF_2 plane). The peak at 930 cm^{-1} with medium intensity and the very weak peaks at 836, 842 and 847 cm^{-1} in band **IV** are also characteristic modes of β-chain PVDF. The 930 cm^{-1} peak corresponds to all of the $-CH_2$ rocking collectively asymmetrical to the symmetry plane of the molecular point group C_s (i.e. a mode having A'' symmetry). The 836, 842 and 847 cm^{-1} modes correspond to all of the $-CH_2$ groups moving asymmetrically in-plane and perpendicular to the

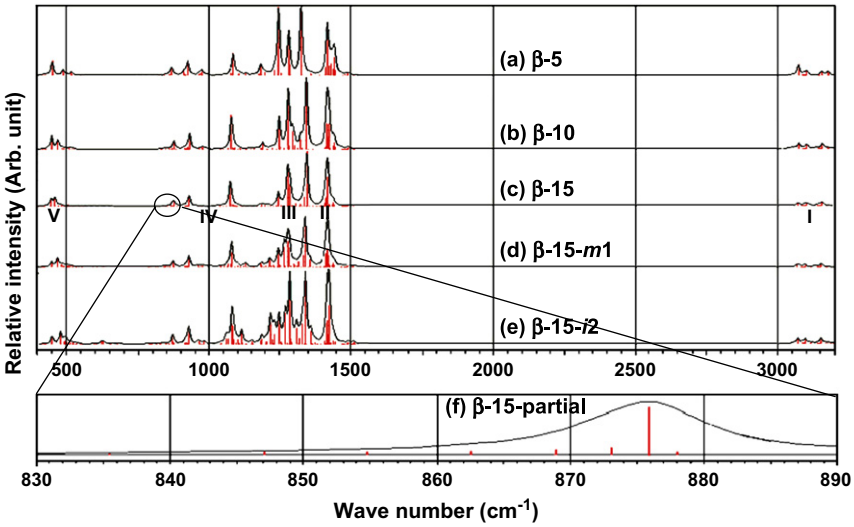

Fig. 9. Calculated IR spectra of β-chain PVDF by B3PW91/6-31G(d): (a) 5 monomer units, (b) 10 monomer units, (c) 15 monomer units, (d) 15 monomer units and one defect located in the *middle* of chain, (e) 15 monomer units and two *isolated* defect in the chain, and (f) partial spectrum of β-chain with 15 monomer units.

polymer chain (Fig. 9(f)). Another medium strong peak at 876 cm^{-1} is also a characteristic mode corresponding to all of the $-CH_2$ groups collectively and symmetrically moving in-plane and perpendicular to the polymer chain in band **IV**, although the wave number is very close to a medium strong peak in the α-phase spectrum in Fig. 8(c) at 877 cm^{-1}. Band **V** has two medium peaks close to each other at 449 and 463 cm^{-1} and one very weak peak at 508 cm^{-1} distinguishable to that in the α-phase (where a single medium intense peak at 490 cm^{-1} was found). The 449 and 463 cm^{-1} modes are from $-CF_2$ and $-CH_2$ in-plane rocking, and the 508 cm^{-1} is from CF_2 scissoring with all of the $-CH_2$ collectively and symmetrically moving in-plane and perpendicular to the polymer chain.

The experimental and theoretical results obtained from different studies show some intrinsic vibrational bands of β-PVDF at 511 (CF_2 bending) [52,55], 840 (CH_2 rocking) [52,55,56] and 1279 cm^{-1} (CF out-of-plane deformation) [30,31,55]. Our calculated frequencies at 508, 836, 847, 876 and 1288 cm^{-1} are consistent with experimental observations except the very weak intensities of the 836 and 847 cm^{-1} modes. The calculations indicate other peaks at 1347, 930, 463 and 449 cm^{-1} are potential references for further identification of the β-PVDF.

Nevertheless, several problems may be encountered in analyzing the spectrum of a given PVDF sample since the preparation of an ideal β-phase PVDF is generally difficult. The spectrum will be largely dependent on molecular mass distribution, head-to-head and tail-to-tail defects, crystalline nature and orientation, thickness of sample, and on the experimental conditions such as sample types and light polarizations. For example, the β-phase spectral data even depended strongly on the diameter of diaphragm [57] in the IR spectrometer and melting process [58].

Fig. 10 shows the simulated Raman spectra of α- and β-chain PVDF with 12 monomer units. It is shown that the spectra are quite different. The peaks for β-PVDF at 876 (all $-CH_2$ collectively and symmetrically moving in-plane and perpendicular to the polymer chain), 1076 (all $-CH_2$ rocking) and 1207 cm^{-1} (C–H twisting) may be characteristic

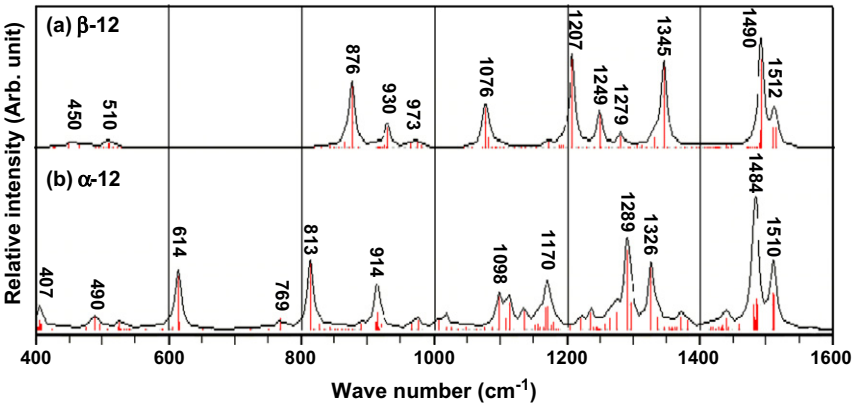

Fig. 10. Simulated Raman spectra of PVDF (with 12 monomer units): (a) β-chain and (b) α-chain.

vibrational modes. The peaks for α-PVDF at 407 (CH_2 wagging out-of-plane), 614 (skeletal bending), 813 ($-CH_2$ rocking) and 1170 cm^{-1} (CH_2 twisting) might also be used for identification.

4. Conclusion and remarks

In this study, DFT-B3PW91/6-31G(d) has been employed to investigate the internal rotation potentials, geometries, relative stabilities, vibrational spectra, dipole moments and mean polarizabilities of the α- and β-chain PVDF. Effects of chain length and monomer inversion defects on the electric properties and vibrational spectra have been discussed. The following are conclusions and remarks derived from our theoretical calculations.

1. The internal rotation potential of the $H(CH_2CF_2)-(CH_2CF_2)H$ model shows that the *tgtg′* conformation between *g* and *g′* angle is about 55° in the α-chain. The β-chain conformation is a slightly distorted all-*trans* alternating planar zigzag with ±175° repeating motif. The α → β transition energy barrier is 16.3 kJ/mol (compared to 10 kcal/mol in literature), and β → α is 8.2 kJ/mol (compared to about 16–17 kJ/mol in literature).
2. In ideal β-chain PVDF, the average distances of the adjacent F atom couples and H atom couples are 2.674 and 2.482 Å, respectively. The average distance of the adjacent monomer unit is 2.567 Å, in good agreement with the experimental value of 2.56 Å from X-ray diffraction. The curvature radii for ideal β-chains containing 6–20 monomer units are almost a constant of about 30.0 Å.
3. The energy difference per monomer unit between β- and α-chains increases with increasing chain length and converges to a nearly constant value of about 10 kJ/mol (compared with 0.3 kcal/mol in literature).
4. Dipole moment contribution per monomer unit in α- and β-chain is 3.81×10^{-30} and 5.01×10^{-30} C m, respectively, for a 20-monomer unit chain. The decrease of dipole moment contribution per monomer with increasing chain length is found mainly due to chain bending. However, chain length does not produce a significant impact on mean polarizability for α- and β-chain PVDF. For a 15-monomer units chain, the mean polarizability per monomer unit in β-chain, 3.63×10^{-40} C m^2 V^{-1}, is slightly higher than the value, 3.56×10^{-40} C m^2 V^{-1}, in α-chain.
5. The molecular dipole moment decreases with increasing defect concentration for both α- and β-chains PVDF, but it is not affected significantly by defect locations in the polymer chain. The presence of inverted monomer units hardly changes the molecular mean polarizability in α-chain, but it will slightly decrease the mean polarizability of β-chain.
6. The calculated IR spectra are in good agreement with experiments. Detailed vibrational assignments were given based on our calculated results. Vibrational bands with potential α- or β-PVDF identification were proposed. The results also show that the invert monomer unit defects in the α- and β-chains will split the peaks and broaden the bands. Calculated Raman spectrum provides more information for the identification of the α- or β-phase PVDF.

Acknowledgments

This work was supported by the National Science Foundation of China (No. 50572089). Part of the calculations was performed in the High Performance Computing Center of Northwestern Polytechnical University.

References

[1] Kawai H. Jpn J Appl Phys 1969;8:975–6.
[2] Lovinger AJ. In: Bassett DC, editor. Developments in crystalline polymers. Englewood, NJ: Applied Science Publishers Ltd.; 1982. p. 195.
[3] Nalwa HS. J Macromol Sci 1991;C31:341–432.
[4] Fukada E. IEEE Trans Ultrason Ferroelectr Freq Control 2000;47(6): 1277–90.
[5] Wang TT, Herbert JM, Glass AM, editors. The applications of ferroelectric polymers. Glasgow and London: Blackies; 1988.
[6] Nalwa HS, editor. Ferroelectric polymers: chemistry, physics and application. New York, Basel, and Hong Kong: Marcel Dekker, Inc.; 1995.
[7] Lovinger AJ. Science 1983;220:1115–21.
[8] Lovinger AJ. Macromolecules 1982;15:40–4.
[9] Sessler GM, editor. Topics in applied physics. Electrets. 2nd ed., vol. 33. Heidelberg: Springer-Verlag; 1987.
[10] Sessler GM. J Acoust Soc Am 1981;70:1596–608.
[11] Inderherbergh J. Ferroelectrics 1991;115(4):295–302.
[12] Nagai M, Nakamura K, Uehara H, Kanamoto T, Takashi Y, Furukawa T. J Polym Sci Part B Polym Phys 1999;37:2549–50.
[13] Strashilov VL. J Appl Phys 2000;88(6):3582–6.
[14] Broahurst MG, Davis GT, McKinney JE, Collins RE. J Appl Phys 1978;49(10):4992–7.
[15] Petchsuk A. Ferroelectric terpolymers, based on semicrystalling VDF/TrTE/chloro-containing termonomers: synthesis, electrical properties, and functionalizations. The Pennsylvania State University; 2003. p. 10, [chapter 1].
[16] Giannetti E. Polym Int 2001;50(1):10–26.
[17] Jungnickel BJ. Poly(vinylidene fluoride) (overview). In: Salamone JC, editor. Polymeric materials handbook. New York: CRC Press Inc; 1999. p. 7115–22.
[18] Lovinger AJ. Polymer 1981;22:412–3.
[19] Pramoda KP, Mohamed A, Phang IY, Liu T. Polym Int 2005;54:226–32.
[20] Dill DR, Tenneti KK, Li CY, Ko FK, Sics I, Hsiao BS. Polymer 2006;47:1678–88.
[21] El Mohajir BE, Heymans N. Polymer 2001;42(13):5661–7.
[22] Sajkiewicz P, Wasiak A, Golclowski Z. Eur Polym J 1999;35(3):423–30.
[23] Gregorio Jr R, Uneo EM. J Mater Sci 1999;34(18):4489–500.
[24] Xu J, Johnson M, Wilkes GL. Polymer 2004;45:5327–40.
[25] lovinger AJ, Davis DD, Cais RE, Kometani JM. Polymer 1987;28: 617–26.
[26] Hasegawa R, Kobayashi M, Tadokoro H. Polym J 1972;3:591–605.
[27] Takahashi N. Jpn J Appl Phys 1996;35:688–93.
[28] Karasawa N, Goddard WA. Macromolecules 1992;25:7268–81.
[29] Li JC, Wang CL, Zhang WL, Yan XX, Wang YX. Acta Phys Sin 2002;51(4):776–81.
[30] Wang CL, Li JC, Zhong WL, Zhang PL. Synth Met 2003;135–136: 469–70.
[31] Li JC, Wang CL, Zhong WL, Zhang PL, Wang QH, Webb JF. Appl Phys Lett 2002;81(12):2223–5.
[32] Farmer BL, Hopfinger AJ, Lando JB. J Appl Phys 1972;43:4293–303.
[33] Correia HMG, Ramos MMD. Comput Mater Sci 2005;33:224–9.
[34] Furukawa T. Phase Transitions 1989;18:143–211.

[35] Tashiro K, Kobayashi M. Phase Transitions 1989;18:213–46.
[36] Hutter J, Luthi HP, Diederich F. J Am Chem Soc 1994;116:750–6.
[37] Li FF, Wu DS, Lan YZ, Shen J, Huang SP, Cheng WD, et al. Polymer 2006;47:1749–54.
[38] Yang L, Feng JK, Ren AM, Sun JZ. Polymer 2006;47:1397–404.
[39] Yang L, Feng JK, Ren AM, Sun CC. Polymer 2006;47:3229–39.
[40] Su KH, Wei J, Hu XL, Yue H, Lü L. Acta Phys Chim Sin 2000;16: 643–51.
[41] Su KH, Wei J, Hu XL, Yue H, Lü L. Acta Phys Chim Sin 2000;16: 718–23.
[42] Lide DR, [editor in chief]. CRC handbook of chemistry and physics. 77th ed. CRC; 1996–1997. p. 9-15–9-23.
[43] Becke AD. J Chem Phys 1992;97:9173–7; Becke AD. J Chem Phys 1993;98:5648–52.
[44] Burke K, Perdew JP, Wang Y. In: Dobson JF, Vignale G, Das MP, editors. Electronic density functional theory: recent progress and new directions. Plenum; 1998. p. 177–97.
[45] Frisch MJ, Trucks GW, Schlegel HB, Scuseria GE, Robb MA, Cheeseman JR, et al. Gaussian 03, Revision B.01. Pittsburgh: Gaussian, Inc.; 2003.
[46] Hehre WJ, Radom L, Schleyer PVR, Pople JA. Ab initio molecular orbital theory. New York: Wiley; 1986. p. 261.
[47] Scott AP, Radom L. J Phys Chem 1996;100:16502–13.
[48] Solymar L, Walsh D. In: Oxford, editor. Lectures on the electric properties of materials. 4th ed. Oxford: Oxford University Press; 1989.
[49] Doll WW, Lando JB. J Macromol Sci Phys 1970;B4:309–29.
[50] Bachmann MA, Lando JB. Macromolecules 1981;14:40–6.
[51] Lando JB, Olf HG, Peterlin A. J Polym Sci Part A-1 Polym Chem 1966;4(4):941–51.
[52] Salimi A, Yousefi AA. Polym Test 2003;22:699–704.
[53] Kobayashi M, Tashiro K, Tadokoro H. Macromolecules 1975;8:158–70.
[54] Tashiro K. Crystal structure and phase transition of PVDF and related copolymers. In: Nalwa HS, editor. Ferroelectric polymers (chemistry, physics, and applications). New York: Marcel Dekker; 1995. p. 74.
[55] Bocaccio T, Bottino A, Capanelli G, Piaggi P. J Membr Sci 2002;210: 315–29.
[56] Gregorio R, Capitao RC. J Mater Sci 2000;35:299–306.
[57] Bormashenko Ye, Pogreb R, Stanevsky O, Bormashenko Ed. Polym Test 2004;23:791–6.
[58] Peng Y, Wu P. Polymer 2004;45:5295–9.